Chemico-Biological Interactions 224 (2014) 24–35

Contents lists available at ScienceDirect

Chemico-Biological Interactions

journal homepage: www.elsevier.com/locate/chembioint

# A flavonoid isolated from *Streptomyces* sp. (ERINLG-4) induces apoptosis in human lung cancer A549 cells through p53 and cytochrome c release caspase dependant pathway

C. Balachandran [a], B. Sangeetha [b], V. Duraipandiyan [a,c,*], M. Karunai Raj [d], S. Ignacimuthu [a], N.A. Al-Dhabi [c], K. Balakrishna [a], K. Parthasarathy [d], N.M. Arulmozhi [e], M. Valan Arasu [c]

[a] Division of Microbiology and Cancer Biology, Entomology Research Institute, Loyola College, Chennai 600 034, India
[b] Department of Toxicology, Advinus Therapeutics Ltd, Bangalore 560058, India
[c] Department of Botany and Microbiology, College of Science, King Saud University, P.O.Box. 2455, Riyadh 11451, Saudi Arabia
[d] Research and Development Centre, Orchid Chemicals and Pharmaceuticals Ltd, Sozhanganallur, Chennai 600119, India
[e] Department of Bioinformatics, Orchid Chemicals and Pharmaceuticals Ltd, Research and Development Centre, Shozanganallur, Chennai 600 119, India

ARTICLE INFO

*Article history:*
Received 21 June 2014
Received in revised form 31 August 2014
Accepted 23 September 2014
Available online 5 October 2014

*Keywords:*
*Streptomyces* sp.
Caspases
Cytochrome c
p53
Molecular docking

ABSTRACT

The aim of this study was to investigate the anticancer activity of a flavonoid type of compound isolated from soil derived filamentous bacterium *Streptomyces* sp. (ERINLG-4) and to explore the molecular mechanisms of action. Cytotoxic properties of ethyl acetate extract was carried out against A549 lung cancer cell line using the 3-(4,5-dimethylthiazol-2-yl)-2,5-diphenyl tetrazolium bromide (MTT) assay. Cytotoxic properties of isolated compound were investigated in A549 lung cancer cell line, COLO320DM cancer cell line and Vero cells. The compound showed potent cytotoxic properties against A549 lung cancer cell line and moderate cytotoxic properties against COLO320DM cancer cell line. Isolated compound showed no toxicity up to 2000 μg/mL in Vero cells. So we have chosen the A549 lung cancer cell line for further anticancer studies. Intracellular visualization was done by using a laser scanning confocal microscope. Apoptosis was measured using DNA fragmentation technique. Treatment of the A549 cancer cells with isolated compound significantly reduced cell proliferation, increased formation of fragmented DNA and apoptotic body. Activation of caspase-9 and caspase-3 indicated that compound may be inducing intrinsic and extrinsic apoptosis pathways. Bcl-2, p53, pro-caspases, caspase-3, caspase-9 and cytochrome c release were detected by western blotting analysis after compound treatment (123 and 164 μM). The activities of pro-caspases-3, caspase-9 cleaved to caspase-3 and caspase-9 gradually increased after the addition of isolated compound. But Bcl-2 protein was down regulated after treatment with isolated compound. Molecular docking studies showed that the compound bound stably to the active sites of caspase-3 and caspase-9. These results strongly suggest that the isolated compound induces apoptosis in A549 cancer cells via caspase activation through cytochrome c release from mitochondria. The present results might provide helpful suggestions for the design of antitumor drugs toward lung cancer treatment.



## 1. Introduction

Cancer is still a major health problem in both developing and developed countries. Cancer, known medically as a malignant neoplasm, is a broad group of various diseases, all involving unregulated cell growth. There are over 200 different known cancers that afflict humans. Every year at least 200,000 people die worldwide from cancer related to their workplace. According to World Health Organization [1] 7.8 million deaths (13% of all deaths) were recorded due to cancer around the world. Deaths from cancer Worldwide are projected to continue to rise to over 13.1 million in 2030. Lung cancer (adenocarcinoma) occurs when there is uncontrolled cell growth in one or both the lungs. Lung cancer is the leading cause of cancer-related deaths in Taiwan, the United States, and other countries. To date the induction of cell death or the inhibition of cell growth using cisplatin, tubulin-binding agents, DNA damaging agents, and UV radiation have

* Corresponding author at: Entomology Research Institute, Loyola College, Nungambakkam, Chennai 600 034, Tamil Nadu, India. Tel.: +91 044 2817 8348; fax: +91 044 2817 5566.
*E-mail address:* avdpandiyan@yahoo.co.in (V. Duraipandiyan).

http://dx.doi.org/10.1016/j.cbi.2014.09.019
0009-2797/

been used to treat lung cancer. Clinically, however, these anticancer agents may result in serious adverse effects including neutropenia, peripheral neuropathy, nephrotoxicity, and chemotherapy resistance. Thus the development of novel chemotherapeutics for lung cancer is warranted. Several anticancer drugs such as Daunomycin, Bleomycins A2 and B2, Dactinomycin, Mitomycin, Rapamycins (RAD001) and Staurosporins (UCN-01, CEP-751) have been derived from *Streptomyces* sp. and are already in clinical use. *Streptomyces* are distributed extensively in soil and provide many important bioactive compounds of high commercial value [2]. Most *Streptomyces* sp. and some other actinomycetes are used in the production of diverse array of antibiotics including aminoglycosides, macrolides, β-lactams, peptides, polyenes, polyether, tetracyclines, etc. *Streptomyces* are also widely recognized as industrially important microorganisms because of their ability to produce many kinds of novel secondary metabolites including antibiotics [3]. Indeed different *Streptomyces* species produce about 75% of commercially and medically useful antibiotics [4,5].

Apoptosis or cell suicide is a highly regulated process that occurs in almost all living cells. It involves the activation of a series of molecular events, leading to cell death that is characterized by cellular, morphological and biochemical changes. These include cell shrinkage, chromatin condensation and nuclear fragmentation, membrane blebbing, caspase activation, and the formation of membrane bound vesicles termed as apoptotic bodies [6,7]. Apoptosis occurs through two main pathways. The first, referred to as the extrinsic or cytoplasmic pathway, is triggered through the Fas death receptor, a member of the tumor necrosis factor (TNF) receptor superfamily [8]. The second pathway is the intrinsic or mitochondrial pathway that when stimulated leads to the release of cytochrome c from the mitochondria and activation of the death signal [9]. Both pathways converge to a final common pathway involving the activation of a cascade of proteases called caspases that cleave regulatory and structural molecules, culminating in the death of the cell. The main pathway that leads to execution of the death signal is the activation of a series of proteases termed caspases. Not all caspases are involved in apoptosis. Caspases are cysteine-aspartic proteases families which play an important role in apoptosis, necrosis and inflammation. Caspases are regulated at a post-translational level ensuring that they can be rapidly activated. The caspases implicated in apoptosis can be further divided into two functional subgroups based on their known or hypothetical roles in the process: initiator caspase (caspases-2, -8, -9, and -10) and effector caspases (caspases-3, -6, and -7). The caspases that have been well described are caspases-3, -6, -7, -8 and -9 [10,11].

The p53 tumor suppressor gene prevents tumourigenesis in response to physiological and environmental stress and plays a role in cell cycle progression, apoptosis and repair of DNA damage. p53 may be involved in transcriptional regulation of pro-apoptotic genes associated with intrinsic and extrinsic pathways [12]. Activated p53 increases the expression of p21 in DNA damaged cells and affects expression of p27 [13–15]. The activation of p53 induces up-regulation of pro-apoptotic Bax but not anti-apoptotic Bcl-2. p53 mediated apoptosis involves the activation of Fas and the intrinsic mitochondrial pathway, which results in activation of caspases-8 and -9 [16,17]. At present there is a need in cancer biology to identify new active chemotherapy drugs which can act as lead compounds for effective drug development. The aim of the present study was to investigate the cytotoxic activity of the total extract from the *Streptomyces* sp. (ERINLG-4) against lung cancer cell line A549. The active principle was also identified. The active principle was also studied for its anticancer activity against A549 lung, COLO320DM cancer cell lines together with normal cell cine viz Vero cells.

## 2. Materials and methods

### 2.1. Isolation and characterization of biological activity of *Streptomyces sp.*

#### 2.1.1. Isolation of *Streptomyces sp.*

The soil samples were collected from the depth of 5–15 cm at Doddabetta forest (Southern Western Ghats), Tamil Nadu, India. Isolation of *Streptomyces* sp. was performed by serial dilution using dilution plate technique. One gram of soil was suspended in 9 mL of sterile distilled water. The dilution was carried out up to $10^{-6}$ dilutions. Aliquots (0.1 mL) of $10^{-2}$, $10^{-3}$, $10^{-4}$, $10^{-5}$ and $10^{-6}$ were spread on the isolation plates containing starch casein agar (Himedia-Mumbai). To minimize the bacterial and fungal growth, actidione (30 mg/L) and nalidixic acid (40 mg/L) were added. The plates were incubated at 28 °C for 7–20 days. The pure colonies were transferred to ISP-2 medium and incubated at 27 °C for 5 days.

#### 2.1.2. Morphological, physiological and biochemical observations

Cultural and morphological features of ERINLG-4 were characterized following the directions given by the International *Streptomyces* Project (ISP) [18] and the Bergey's Manual of Systematic Bacteriology. Cultural characteristics of pure isolates in various media (ISP 1–7) were recorded after incubation at 28 °C for 7–14 days. Morphology of spore bearing hyphae with entire spore chain was observed with a light microscope (Model SE; Nikon) using cover-slip method in ISP medium (ISP 3–6). The shape of cell, Gram-stain, color determination, the presence of spores, and colony morphology were assessed on solid ISP agar medium. Biochemical reactions, different temperatures, NaCl concentration, pH level, pigment production, enzyme reaction and acid or gas production were done following the methods of Balachandran et al. [19] and Balachandran et al. [20].

#### 2.1.3. 16S rRNA gene amplification

Genomic DNA of ERINLG-4 was isolated by the methods of Hipura *Streptomyces* DNA spin kit-MB 527-20pr from Hi-media. The 16 S ribosomal RNA gene was amplified by PCR method using primers 27f ($5^1$AGTTTGATCCTGGCTCAG$3^1$) and 1492r ($5^1$ACGGCTACCTTG TTACGACTT$3^1$). Each PCR mixture in a final volume of 20 μL contained 10 mM Tris–HCl (pH.8.3), 50 mM KCl, 1.5 mM $MgCl_2$, 200 μM of each dNTP, 10 pmol of each primer, 50 ng of genomic DNA and 1U of Taq DNA Polymerase (New England Biolabs. Inc). The conditions for thermal cycling were as follows: denaturation of the target DNA at 94 °C for four minutes followed by 30 cycles at 94 °C for 1 min, primer annealing at 52 °C for one minute and primer extension at 72 °C for 1 min. At the end of the cycling, the reaction mixture was held at 72 °C for 10 min and then cooled to 4 °C. PCR amplification was detected by 1% agarose gel electrophoresis and was visualized by ultraviolet (UV) fluorescence after ethidium bromide staining. The PCR product obtained was sequenced by an automated sequencer (Genetic Analyser 3130, Applied Biosystem, and USA). The same primers as above were used for this purpose. The sequence was compared for similarity with the reference species of bacteria contained in genomic database banks using the NCBI BLAST available at http://www.ncbinlm-nih.gov/.

#### 2.1.4. Nucleotide sequence accession number

The partial 16S rRNA gene sequences of isolate ERINLG-4 have been deposited in the GenBank database under accession number HQ385920. A phylogenetic tree was constructed using the neighbor joining DNA distance algorithm using software MEGA (version 4.1) [21].

*2.1.5. Extraction*

Culture inoculate of the isolate ERINLG-4 was taken in 500 mL Erlenmeyer flasks containing 150 mL of fermentation medium containing Glucose-10 g, Starch-24 g, Peptone-3.0 g, Meat extract-3.0 g, Yeast extract-5.0 g, $CaCO_3$-4.0 g, pH-7 and $H_2O$-1L. Culture inoculates were incubated at different temperature (20, 25, 30, 35, 40, 45 and 50 °C), different pH (pH 1, 3, 5, 7, 9 and 11), different days (2, 4, 6, 8 and 10 days) and different concentrations (300, 250, 200, 150, 100, and 50 μg/mL) in a shaker (200 rpm) for 10 days. After 10th day the culture broth was centrifuged at 8000g for 20 min to remove the biomass. Equal volume of ethyl acetate (1:1 v/v) was added. The extract was evaporated to dryness at 40 °C under reduced pressure.

*2.1.6. Cell lines*

Human A549 lung adenocarcinoma cancer cell line, COLO320DM adenocarcinoma colon cancer cell line and Vero cells (Normal cell line) were obtained from National Institute of Cell Sciences, Pune, India.

*2.1.7. Cytotoxic properties of extracts*

Cytotoxic properties of ethyl acetate extract were studied against A549 lung adenocarcinoma cancer cell. A549 cell line was maintained in complete tissue culture medium (Dulbecco's Modified Eagle's Medium) with 10% Fetal Bovine Serum and 2 mM L-Glutamine, along with antibiotics (about 100 International Unit/mL of penicillin, 100 μg/mL of streptomycin) with the pH adjusted to 7.2. The cytotoxicity was determined according to the method of Balachandran et al. [22] with some changes. Cells (5000 cells/well) were seeded in 96 well plates containing medium with different concentrations of ethyl acetate extract. The cells were cultivated at 37 °C with 5% $CO_2$ and 95% air in 100% relative humidity. After various durations of cultivation the solution in the medium was removed. An aliquot of 100 μL of medium containing 1 mg/mL of 3-(4,5-dimethylthiazol-2-yl)-2,5-diphenyl-tetrazolium bromide (MTT) was loaded in the plate. The cells were cultured for 4 h and then the solution in the medium was removed. An aliquot of 100 μL of DMSO was added to the plate which was shaken until the crystals were dissolved. The cytotoxicity against cancer cells was determined by measuring the absorbance of the converted dye at 540 nm in an ELISA reader. Cytotoxicity of each sample was expressed as $IC_{50}$ value. The $IC_{50}$ value is the concentration of test sample that causes 50% inhibition of cell growth averaged from three replicate experiments.

*2.1.8. Isolation of active principle*

The active ethyl acetate extract was fractionated (15 g) using silica gel column chromatography. The total ethyl acetate extract was chromotographed over silica gel (Merck 60–120 mesh, 1750 g, 3.5 i.d. × 150 cm) packed with chloroform. The column was successively eluted with chloroform, chloroform–ethyl acetate mixtures with increasing polarity with ethyl acetate, ethyl acetate–methanol and methanol. Based on thin layer chromatography (TLC) profiles, the fractions were combined to give 21 fractions. When the fractions were bioassayed fraction 17 showed good cytotoxic activity. Elusion of the column with ethyl acetate: methanol (3:1) gave compound as pale yellow gummy residue which was purified by preparatory HPLC. The fraction 17 was subjected to preparative HPLC analyses performed with an Isocratic elution capability (Waters Alliance System). The column (length 250 mm, internal diameter 6.0 mm) was filled with porous silica particles of 15 μ diameter bonded with octadecylsilane (YMC pack ODS A (250 × 6.0 mm), 15 μ). The mobile phase was composed of acetonitrile and aqueous acetic acid (15:85, v/v); it was isocratically eluted at a flow-rate of 3 mL/min and injection volume was 100 μL. Elution was monitored at 254 nm and peak fraction was collected according to the elution profile.

*2.1.9. In vitro anticancer activity of isolated compound*

As given in Section 2.1.7.

*2.2. Cellular and biochemical mechanisms of apoptosis*

*2.2.1. DNA fragmentation*

For the DNA fragmentation assay A549 lung adenocarcinoma cancer cells ($1 \times 10^6$ cells) (control and treated with isolated compound) were collected by centrifugation at 2000 rpm for 10 min and washed twice with phosphate-buffered saline (PBS, Ambion USA). The cell pellet was suspended in 100 μL of cell lysis buffer (10 mM Tris–HCl buffer, pH 7.4 containing 10 mM EDTA and 0.5% triton X-100), kept at 4 °C for 15 min and the cell lysate was centrifuged at 16,000 rpm for 20 min. The supernatants were incubated with proteinase K (0.4 mg/mL; Sigma–Aldrich) at 60 °C for 60 min, then incubated with RNase A (0.4 mg/mL; Sigma–Aldrich) at 37 °C for 60 min. The supernatants were mixed with 20 μL of 5 M NaCl and 120 μL of isopropyl alcohol overnight at −20 °C. The supernatants were then collected by centrifugation at 16,000 rpm for 15 min. DNA samples were dissolved in TE buffer (10 mM Tris–HCl, pH 7.4 and 1 mM EDTA, pH 8.0), and separated by 2% agarose gel electrophoresis [23].

*2.2.2. Confocal microscopy*

A549 cells were cultured in medium supplemented with or without compound (164 μM). After 24 h of treatment, cells were washed twice with 0.01 M PBS and suspended in binding buffer. Cells were incubated with FITC and PI for 30 min at 4 °C in the dark room. Cells were then centrifuged and pellets were smeared. FITC (Fluorescein Isothiocyanate) and PI (Propidium Iodide) fluorescence was immediately observed under confocal laser scanning microscope (Olympus, FV1000, Japan) at 400× magnifications [24].

*2.2.3. Reverse transcriptase polymerase chain reaction (RT-PCR)*

Total RNA from A549 cancer cells was isolated using ONE STEP-RNA Reagent (Biobasic Inc.). It is a ready to use reagent for the isolation of total RNA from cells. The reagent, a mono-phasic solution of phenol and guanidine isothiocyanate, is an improvement to the single-step RNA isolation method developed by Chomczynski and Sacchi [25]. The following gene specific oligonucleotide primers were used for the generation of cDNAs. The sequences of the primers used were: p53f-5′ TCTGTGACTTGCACGTACTC 3′, p53r-5′ CACGGATCTGAAGGG TGAAA 3′, Caspase-3f -5′ TGGAGCGAATCAAT GGACT 3′, Caspase-3f-5′ AGGACTCAAT TCTTGCCAC 3′, Caspase-9f-5′ GCT CTT CCT TTG TTC ATC TCC 3′ and Caspase-9r-5′ CAT CTG GCT CGG GGT TAC TGC 3′ and GAPDH f-5′ TCCCATCACCATCT TCCA 3′, GAPDH r-5′ CATCACGCCACAGTTTCC 3′. PCR products were visualized on a 2% agarose gel. Glyceraldehyde-3-phosphate dehydrogenase (GAPDH) is one of the most commonly used housekeeping gene for comparisons of gene expression data [26]. GAPDH was simultaneously amplified along with the respective genes to confirm uniformity of RNA concentration taken for the expression studies.

*2.2.4. Western blotting*

Treated or non-treated (24 h) A549 lung adenocarcinoma cancer cells were collected by centrifugation at 2500 rpm for 5 min and washed twice with PBS and lysed in ice-cold radio immunoprecipitation buffer (RIPA) after addition of protease inhibitors. The amounts of proteins in the samples were quantified using Bradford's assay. The samples were subjected to sodium dodecyl sulfate–polyacrylamide gel electrophoresis (SDS–PAGE) with 13% resolving gel. After SDS–PAGE it was transferred to nitrocellulose

membrane. Membranes were blocked with blocking buffer (Tris-buffered saline, i.e., TBS, containing 5% non-fat milk) for 1 h at room temperature. Membrane was incubated overnight at 4 °C with the following specific primary antibodies: Bcl-2 (C 21, SC783 – rabbit polyclonal), p53 (FL393 – rabbit polyclonal), caspase-3 (SC7148 – rabbit polyclonal), caspase-9 (SC7885 – rabbit polyclonal), cytochrome c (SC7159 – rabbit IgG) and GAPDH (FL-335 – rabbit polyclonal antibody) (Santa Cruz Biotechnology, Santa Cruz, USA) with dilution of 1:1000–2000. Further incubation with appropriate horseradish peroxidise conjugated secondary antibodies (Sigma), depending on the primary antibody used, was performed for 1 h at room temperature. Detection of staining signals was captured by using chem-documentation system after enhancing them with chemiluminescence kit (Pierce Biotech) [23].

#### 2.2.5. Toxicity study

Toxicity study was tested against normal Vero cells. Vero cell line was maintained in complete tissue culture medium (DMEM) with 10% Fetal Bovine Serum and 2 mM L-Glutamine, along with antibiotics (about 100 International Unit/mL of penicillin, 100 μg/mL of streptomycin) with the pH adjusted to 7.2. The toxicity was determined according to the method of Balachandran et al. [22]. The different concentrations of isolated compound were tested against Vero cell line (10–2000 μg/mL).

### 2.3. Molecular docking studies

#### 2.3.1. Protein selection

Three dimensional structures of Cellular tumor antigen caspases-3 (PDB ID: 1QX3) and caspase-9 (PDB ID: 1JXQ) were retrieved from the Protein Data Bank (PDB) http://www.pdb.org. The water molecules were removed and the hydrogen bonds were added to the whole structure molecules.

#### 2.3.2. Binding active site prediction

The probable binding sites of preferred target receptors were searched using Q-site Finder to predict the ligand binding site. It works by binding hydrophobic ($CH_3$) probes to the protein, and finding clusters of probes with the most favorable binding energy. These consist of active sites on protein surfaces and voids covered in the interior of proteins. The individual probe sites relate most closely to the favored high-affinity binding sites on the protein surface. These favorable binding sites relate to locations where a putative ligand could bind and optimize its van der Waals interaction energy. Q-site Finder includes a graphical user interface, flexible interactive visualization, as well as on-the fly computation for user uploaded structures. It is important to keep the predicted ligand binding site as small as possible without compromising accuracy for a range of applications such as molecular docking, *de novo* drug design and structural identification and comparison of functional sites [27].

#### 2.3.3. Docking analysis

Molegro virtual docker was used to predict potential binding site on caspases-3 and caspases-9. Based on the cavities detected the isolated molecule was docked with the active site amino acids. The docking was performed using Molegro Virtual Docker (MVD). The MolDock scoring function used by MVD is derived from the PLP scoring functions originally proposed by Gehlhaar et al. [28] and later extended by Yang et al. [29]. The MolDock scoring function further improves these scoring functions with a new hydrogen bonding term and new charge schemes. The docking search algorithm (MolDock Optimizer) used in MVD is based on an evolutionary algorithm [30]. Evolutionary algorithms (EAs) are iterative optimization techniques inspired by Darwinian evolution theory. In EAs the evolutionary process is simplified and thus it has very little in common with real world evolution. Nevertheless, during the last fifty years EAs have proved their worth as powerful optimization techniques that can assist or replace traditional techniques when these fail or are inadequate for the task to be solved.

### 2.4. Statistical analysis

Anticancer activities of quercetin-3-O-β-L-rhamnopyranosyl-(1 → 6)-β-D-glucopyranoside were statistically analyzed by Duncan multiple range test at $P = 0.05$ with the help of SPSS 11.5 version software package.

## 3. Results and discussion

### 3.1. Isolation and characterization of Streptomyces sp.

#### 3.1.1. Morphology and biochemical studies

The *Streptomyces* sp. isolate ERINLG-4 was recovered from Doddabetta forest soil in Nilgiris (Southern Western Ghats), Tamil Nadu, India. The strain was Gram-positive filamentous bacterium. The culture characteristics of the new isolate were observed after 7, 14 and 21 days of incubation on different media. The color of the substrate mycelia was yellow. The spore chains were white. These characteristic morphological properties strongly suggested that ERINLG-4 isolate belonged to *Streptomyces* genus. *Streptomyces* sp. (ERINLG-4) showed good growth on medium amended with sodium chloride up to 8%; no growth was seen at 10%. Permissive temperature for growth ranged from 25 to 37 °C with optimum of 30 °C and the pH range was 6–10 with normal pH of 7. Utilization of various carbon sources by ERINLG-4 indicated a wide pattern of carbon source assimilation. Lactose, galactose, arabinose, rhamnose and ribose did not support the growth of the isolate (Table 1). Gram staining, morphology and cultural characteristics of *Streptomyces* sp. isolate ERINLG-4 indicated that it was Gram positive, aerobic and grew well in all media. The cultural characteristics and morphological characteristics of different *Streptomyces* isolates have been reported by several investigators [31].

#### 3.1.2. 16S rRNA gene amplification

The result of the sequencing of ERINLG-4 was obtained in the form of rough electrophoregrams. The total nucleotide sequence was 1513 bp (bp-1513: 341A, 383C, 513G and 276T). The sequences have been chosen as reference sequences in which unidentified and unpublished sequences were not included. Alignment of this sequence through matching with reported 16S rRNA gene sequences in the GenBank showed high similarity to *Streptomyces* 16S rRNA genes. The sequences were blasted via NCBI Blast software for comparison with the homologous sequences contained in the data bank (GenBank). The sequence results revealed that isolate ERINLG-4 was *Streptomyces* sp. Clustering analysis obtained by the MEGA4 method showed that the isolate ERINLG-4 was taxonomically very close to *Streptomyces caelestis*. The phylogenetic tree obtained by applying the neighbor joining method is illustrated in Fig. 1. Cultural characteristics and 16S rRNA studies strongly suggested that this isolate belonged to the genus *Streptomyces*. Studies on the microbial diversity by 16S rRNA gene analysis showed that a group of high-GC Gram-positive bacteria (actinomycetes) are dominant in the soil [32]. The universal primers seem to be sufficient for identifying the genus but not the species.

#### 3.1.3. Cytotoxic properties of ethyl acetate extract

Ethyl acetate extract showed good cytotoxic activity *in vitro* against A549 lung adenocarcinoma cancer cell line. Ethyl acetate extract was taken from *Streptomyces* sp. (ERINLG-4) in different

**Table 1**
Physiological and biochemical characteristics of *Streptomyces* sp. isolate ERINLG-4.

| Characteristics | Results |
|---|---|
| Gram staining | Positive |
| Shape and growth | Filamentous aerial growth |
| Range of temperature for growth | 25–37 °C |
| Optimum temperature | 30 °C |
| Range of pH for growth | 6–10 |
| Normal pH | 7 |
| Amylase | + |
| Chitinase | – |
| Protease | + |
| Gelatinase | – |
| Indole production | + |
| Growth in the presence of NaCl | 1–8% |
| *Sugar analysis* | |
| Mannose | + |
| Maltose | + |
| Lactose | – |
| Sucrose | + |
| Glucose | + |
| Galactose | – |
| Starch | + |
| Mannitol | + |
| Arabinose | – |
| Xylose | + |
| Rhamnose | – |
| Ribose | – |
| **Standard antibiotics** | **Sensitivity** |
| Ciprofloxacin | S |
| Gentamicin | S |
| Ampicillin | S |
| Cephaloridine | S |
| Streptomycin | S |
| Erythromycin | S |
| Vancomycin | S |
| Amikacin | S |
| Penicillin | S |
| Rifamycin | S |
| Norfloxacin | S |

+: presence; –: absence.

concentrations, different days of incubations, different pH and different temperatures. Different concentrations of ethyl acetate extract were taken and tested for cytotoxic activity against A549 cancer cell line; it showed 88.31% activity at the dose of 300 μg/mL with $IC_{50}$ value of 200 μg/mL (Fig. 2A). When the different days incubations were studied 10th day extraction showed good cytotoxic activity compared to other days. The activity was gradually increasing day by day (Fig. 2B). Ethyl acetate extract was extracted from different pH conditions. Particularly pH-7 showed good cytotoxic activity at the dose of 300 μg/mL with $IC_{50}$ value of 200 μg/mL compared to other pH conditions (Fig. 2C). Optimum temperature of 30 °C showed good cytotoxic activity (86.19%) at the dose of 300 μg/mL with $IC_{50}$ value of 200 μg/mL (Fig. 2D). The ethyl acetate extract taken from *Streptomyces* sp. (ERINLG-4) in fermentation medium with an optimum temperature of 30 °C, pH-7 and 10th of day incubation was suitable for the isolation of the active compound.

### 3.1.4. Isolation of quercetin-3-O-β-L-rhamnopyranosyl-(1 → 6)-β-D-glucopyranoside

The pure compound was obtained as pale yellow gummy residue (Yield-155 mg). The purity of the isolated compound was analyzed using High-performance liquid chromatography. The compound gave a single spot on TLC over silica gel with ethyl acetate: methanol (1:1) as the developing system (Rf-0.62). The pale yellow spot turned dark yellow on exposure to ammonia vapor. The compound answered positive for ferric reaction. It also answered for anthrone sulfuric acid test for sugar by giving dark green color. It also gave positive result for flavonoids in shinoda test (reddish pink color with Mg/HCl). Molecular formula is $C_{27}H_{30}O_{16}$, ESI-MS, *m/z* 575 $[M+H-2H_2O]^+$, UV: $\lambda_{max}$ MEOH nm 250, 266, 287 and 375. IR: $\upsilon_{max}$KBr $CM^{-1}$: 3395 (hydroxyl), 2960, 1660 (flavonoid carbonyl), 1412, 1234, 1109, 756, 636. $^1H$ NMR (δ, $CD_3OD$, 400 MHz): 1.15 (3H, d, *J* = 6.4 Hz, rhamnose methyl), 3.20–3.85 (9H, sugar protons), 4.54 (1H, d, *J* = 1.6 Hz, H-1‴), 5.13 (1H, d, *J* = 7.6 Hz, H-1″), 6.23 (1H, d, *J* = 2.0 Hz, H-6), 6.42 (1H, d, *J* = 2.0 Hz, H-8), 6.90 (1H, d, *J* = 8.8 Hz, H-5′), 7.64 (1H, dd, *J* = 8.8

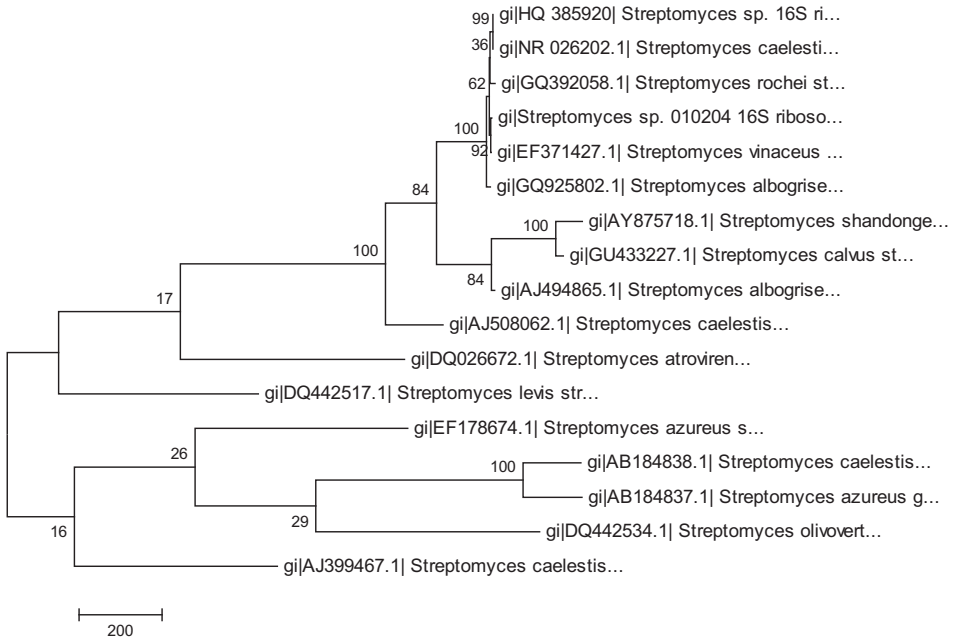


**Fig. 1.** Phylogenetic tree derived from 16S rRNA gene sequences showing the relationship between isolate ERINLG-4 and species belonging to the genus *Streptomyces* constructed using the neighbor-joining method. Bootstrap values were expressed as percentages of 1000 replications.

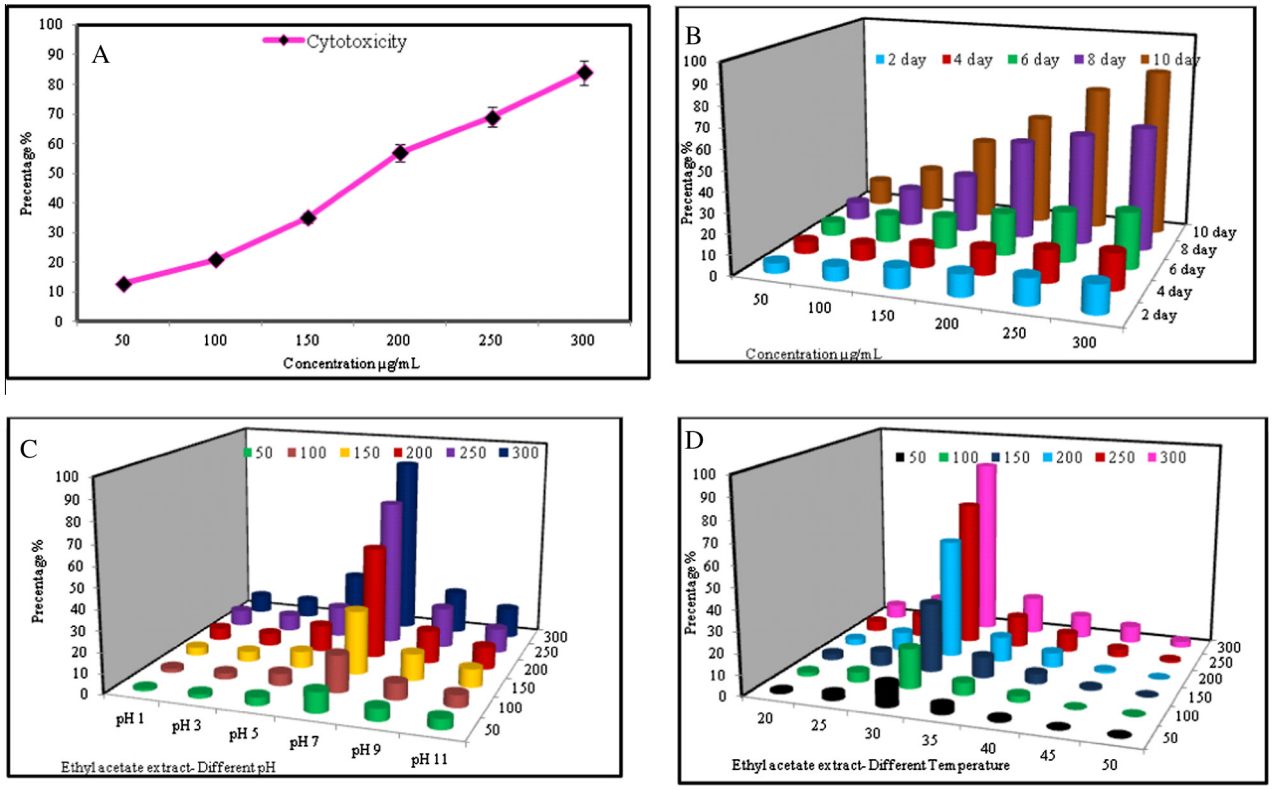


**Fig. 2.** Cytotoxic effects of ethyl acetate extract obtained from *Streptomyces* sp., (ERINLG-4) against A549 cancer cell line. (A) Different concentration of ethyl acetate extract (10th day ethyl acetate extract), (B) incubation at different days, (C) incubation at different pH (10th day ethyl acetate extract) and (D) incubation at different temperature (10th day ethyl acetate extract).

and 2.4 Hz, H-6′), 7.69 (1H, d, $J$ = 2.4 Hz, H-2′). $^{13}$C NMR (δ, $CD_3OD$, 100 MHz): 158.52 (C-2), 135.65 (C-3), 179.49 (C-4), 162.99 (C-5), 99.96 (C-6), 166.02 (C-7), 94.88 (C-8), 159.53 (C-9), 105.65 (C-10), 123.15 (C-1′), 116.07 (C-2′), 145.80 (C-3′), 149.81 (C-4′), 117.72 (C-5′), 123.58 (C-6′), 102.43 (C-1″), 73.96 (C-2″), 75.75 (C-3″), 69.72 (C-4″), 77.23 (C-5″), 68.57 (C-6″), 104.73 (C-1‴), 72.12 (C-2‴), 72.26 (C-3‴), 71.12 (C-4‴), 71.44 (C-5‴), 17.89 (C-6‴) (Fig. 3). IR spectrum showed hydroxyl 3395 cm$^{-1}$ and α, β unsaturated chelated carbonyl at 1660. On acid hydrolysis with 5% alcoholic hydrochloric acid on a water bath (2 h) it gave glucose and rhamnose as identified by paper chromatography. The $^1$H and $^{13}$C NMR spectra of isolated compound clearly showed the compound to be isomeric with rutin with the terminal sugar unit being β-L-rhamnose instead of α-L rhamnose. This was confirmed by comparison of the $^1$H and $^{13}$C NMR values with those of rutin. H-6 and H-8 the two meta-couple protons appeared as one proton doublets ($J$ = 2.0 Hz) at delta 6.23 and 6.42 respectively. H-2′ in ring B appeared as one proton doublets ($J$ = 2.4 Hz) at delta 7.69. H-5′ appeared as ortho-coupled doublet ($J$ = 8.8 Hz), at delta 6.9. H-6′ appeared as one proton double doublets at delta 7.64 ($J$ = 8.8 and 2.4 Hz). The anomeric hydrogen H-1" of glucose appeared as doublet ($J$ = 7.6 Hz) at delta 5.13. The anomeric hydrogen H-1‴ of rhamnose appeared as one proton doublet ($J$ = 1.6 Hz) at delta 4.54. The value was slightly up field when compared with that of rutin where H-1‴ appeared at delta 5.12 as a doublet ($J$ = 1.9 Hz). This is because of the inversion of configuration at C-1‴ due to change of terminal sugar moiety from α-L-rhamnose to β-L-rhamnose. In the $^{13}$C NMR spectrum C-1‴ appears down field at delta 104.74 instead of delta 100.9 as in rutin. Similarly C-3‴ and C-5‴ are also moved down field. The rhamnose methyl appeared as three proton doublet ($J$ = 6.4 Hz) at delta 1.15. The remaining nine sugar protons appeared in the region delta 3.02–3.85. The HMBC spectrum H-1″ of glucose (delta 5.13) showed correlation with C-3 (delta 135.65) of the flavones unit. Similarly H-1‴ (delta 4.54) showed correlation with C-6″ of glucose at delta 68.57. This showed that the sugar unit was attached to C-3 of the aglycone quercetin. Thus the structure of the compound was confirmed to be quercetin-3-O-β-L-rhamnopyranosyl-(1 → 6)-β-D-glucopyranoside. The compound did not correspond to authentic rutin on TLC over silica gel and was found to be more polar as given above. Only two reports were available in the website; these two studies have not reported the spectroscopic and biological data [33].

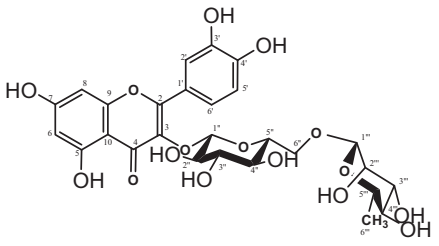

**Fig. 3.** Structural representation of the compound quercetin-3-O-β-L-rhamnopyranosyl-(1 → 6)-ββ-D-glucopyranoside.

### 3.1.5. Cytotoxic properties of isolated compound

Quercetin-3-O-β-L-rhamnopyranosyl-(1 → 6)-β-D-glucopyranoside isolated from *Streptomyces* sp. (ERINLG-4) were tested against A549 lung cancer cell line, COLO320DM cancer cell line and Vero cell line (Normal cell). The isolated compound showed prominent cytotoxic activity against A549 lung cancer cell line. The compound showed 87.41% activity at the dose of 164 µM with $IC_{50}$ value of 82 µM. COLO320DM cancer cell line was maintained in complete

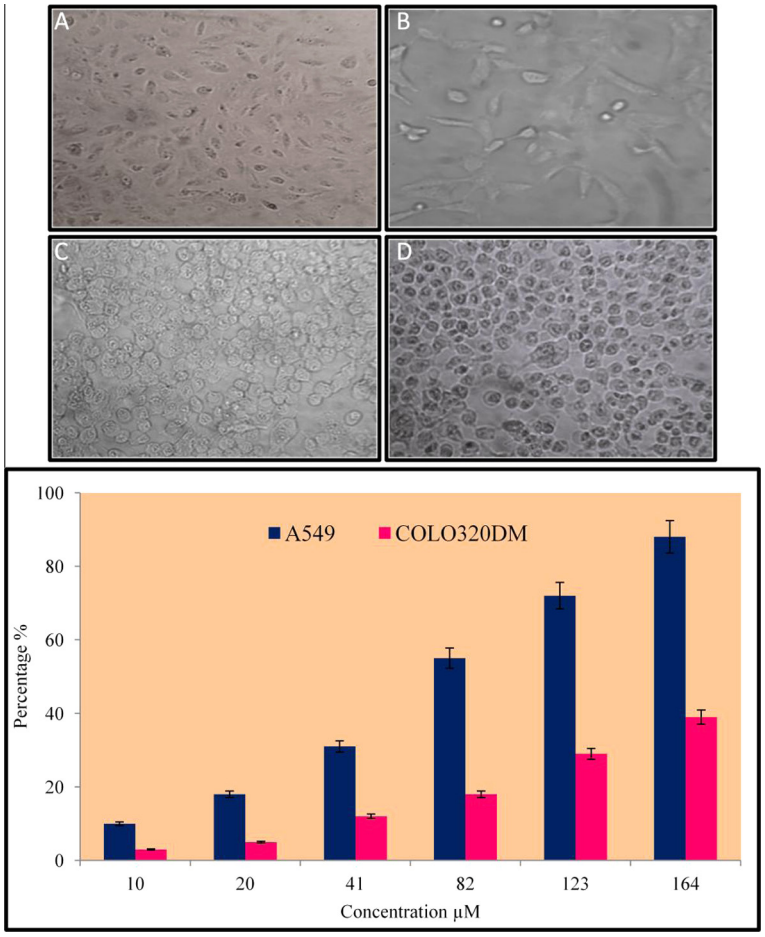


**Fig. 4.** Cytotoxic effects the compound against cancer cell line (A549) (A +ve) and (B −ve) control cells; (C) and (D) treated cells. Data are mean ± SD of three independent experiments with each experiment conducted in triplicate. Isolated compound showed moderate activity against tested COLO320DM cancer cell line. Positive control 9.80 ± 0.43 µM ($IC_{50}$) (Cisplatin).

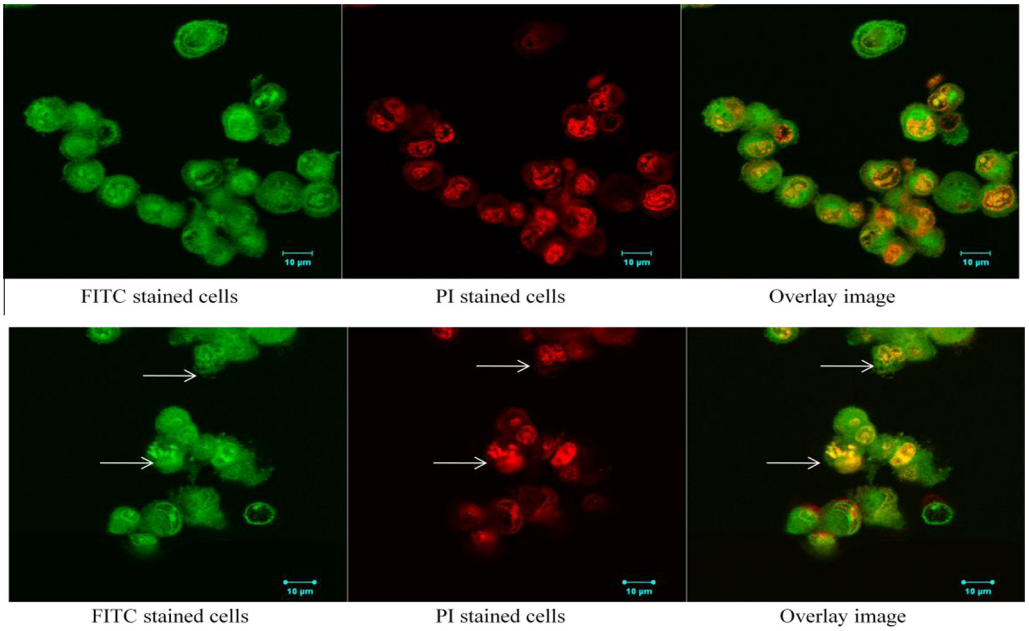


**Fig. 5.** FITC and PI triple fluorescence staining for the detection of apoptosis in A549 cell. Cell was treated with 164 µM at 24 h. The fluorescent signals of FITC and PI were examined under confocal laser scanning microscope. (A) Control and (B) compound treated apoptotic cancer cells. Arrows indicate apoptotic cancer cells.

tissue culture medium (Roswell Park Memorial Institute) and the compound showed moderate cytotoxic property (Fig. 4). All concentrations used in the experiment decreased the cell viability significantly ($P < 0.05$) in a concentration dependent manner. Isolated compound showed no toxicity against Vero normal cell line up to 2000 μg/mL (data not shown). The isolated compound showed potent cytotoxic activity against A549 lung cancer cell line compared to COLO320DM cancer cell line. So we have concentrated on the anticancer activity against A549 cancer cell line only. Previously many studies have been reported flavonoid type of compounds with good cytotoxic activity against cancer cell lines [34–37].

### 3.2. Cellular and biochemical mechanisms of apoptosis

#### 3.2.1. Confocal microscopic studies

Confocal microscopic study showed apoptosis or morphological changes in isolated compound treated cells (Fig. 5). We also judged cell apoptotic status by FITC and PI triple fluorescence staining. FITC acts as a phosphatidyl serine tracer and suggests the presence of apoptosis. PI can only penetrate cells where the cell membrane has been compromised.

#### 3.2.2. Effect of flavonoid on DNA fragmentation of A549 lung cancer cells

DNA fragmentation was demonstrated by incubating A549 cells with different concentrations of isolated compound for 24 h. DNA fragmentation became apparent with 123 and 164 μM compound treatment and this DNA fragmentation response was dose dependent (Fig. 6). When cells were treated with 123 and 164 μM DNA ladders were visible from 24 h after treatment. Previously flavonoid type of compounds such as apigenin, quercetin and myricetin showed good DNA fragmentation pattern [38].

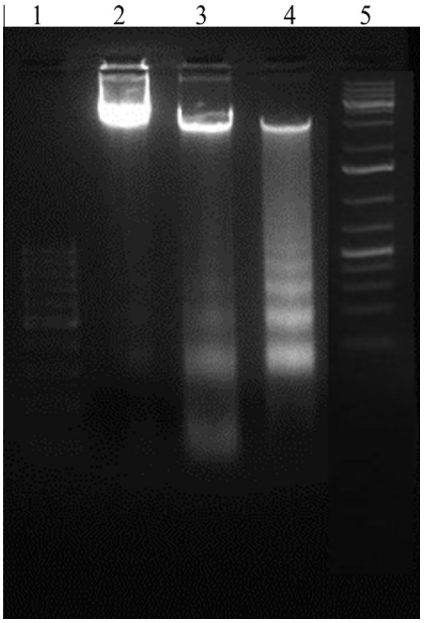


**Fig. 6.** Detection of DNA fragmentation by agarose gel electrophoresis. The apoptotic DNA fragmentation was detected by agarose gel electrophoresis in A549 cancer cells treated with compound for 24 h lane-3 123 μM and lane-4 164 μM, compared to DNA from untreated samples (lane 2). lane-1 100 bp DNA ladder marker and lane-5 1kp DNA ladder marker.

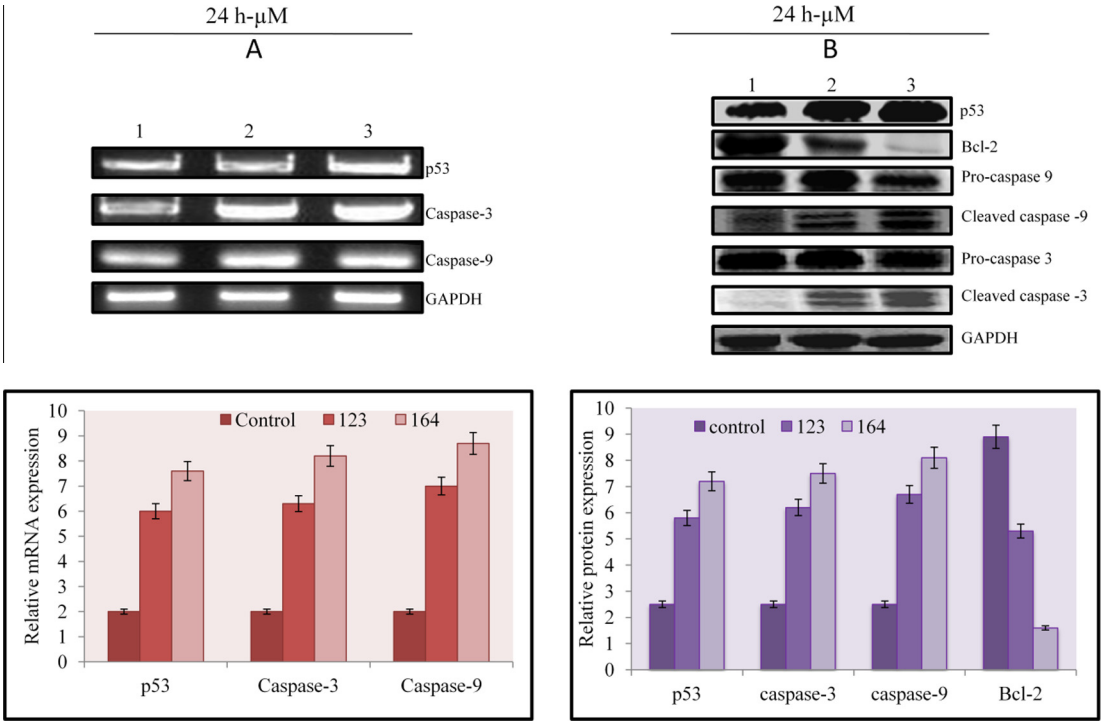


**Fig. 7.** (A) Expression of pro and anti-apoptotic genes of p53, caspase-3 and caspase-9 in A549 cells following exposure to flavonoid for 24 h. Cells were plated on T75 flasks and after 24 h they were treated with different concentrations of flavonoid. After flavonoid treatment cells were harvested and RNA was isolated. RT-PCR was performed as described in Section 2. PCR products were resolved on a 2% agarose gel and visualized using ethidium bromide. Column-1 control cells; Column-2 123 μM and Column-3 164 μM. GAPDH was used as an internal control. (B) Activation of p53, Bcl-2, pro-caspases, cleaved caspases and cytochrome c lung cancer cells by flavonoid. Western blotting analysis of Bcl-2, pro-caspases, cleaved caspases, p53 and cytochrome c after flavonoid treatment at different concentrations of 123 and 164 μM for 24 h; total cell lysates were prepared by a RIPA buffer and Western blotting was performed using suitable antibodies against Bcl-2, caspase-9, caspase-3, p53 and cytochrome c. Column-1 control cells; Column-2 123 μM and Column-3 164 μM. GAPDH was used as an internal control. *$P < 0.05$ compared to flavonoid treated A549 cells.

*3.2.3. Activation of p53*

The pro-apoptotic pathway associated with compound treatment, namely the expression of p53 in A549 cells treated with 123 and 164 μM concentration of compound for 24 h, was tested by RT-PCR and western blotting analysis. Compared to the control, cells treated with isolated compound were strongly up-regulated at mRNA and protein level (Fig. 7A and B). p53 protein does not directly participate in the apoptosis pathway; however, it regulates a host of other genes that lead to cell arrest or apoptosis. The p53 protein has been implicated in several growth related pathways, including promoting oxidative metabolism and down-regulating glycolysis [39]; there are several observations that p53 directly impacts mitochondrial function and structural integrity in the context of apoptosis. Several apoptotic stimuli provoke a rapid translocation of p53 to the outer mitochondrial membrane [40]. p53 also participates in apoptosis induction by acting directly at mitochondria. Localization of p53 to the mitochondria occurs in response to apoptotic signals and precedes cytochrome c release and procaspase-3 activation. Caspase-9 and caspase-2 respond to changes in mitochondrial potential; p53 boosts the activation of the caspase cascade by both transcription dependent and independent mechanisms. Caspase-9 has been shown to execute p53-dependent radiation induced apoptosis.

*3.2.4. Effect of isolated compound on caspase activity and cytochrome c release of A549 cells*

Caspases are a family of cysteine proteases that are activated during the execution phase of the apoptotic process. Once activated caspases cleave and activate downstream caspases. We focused on the activation of caspase-3 and caspase-9 which are known to play an important role in the formation of apoptotic bodies. Treatment of the cells with compound induced caspase-3 and caspase-9 activities in a concentration dependent manner which was confirmed by mRNA and western blot analysis. The mitochondria mediated apoptotic pathway related to gene expression of caspase-3 and caspase-9 in A549 cells treated with the 123 and 164 μM concentrations of isolated compound for 24 h was tested by RT-PCR analysis (Fig. 7A). To determine the signal pathway of A549 cell apoptosis by isolated compound, following incubation with the 123 and 164 μM concentrations of compound for 24 h, protein expression of Bcl-2, pro-caspases, caspase-3, caspase-9 and cytochrome c activation were confirmed by western blotting analysis. Compound significantly increased cleavage of caspase-3 and caspase-9 at 24 h. The increase of cleaved caspase-3 and caspase-9 was associated with the decrease of pro-caspase-3 and pro-caspase-9. Caspase-3 and caspase-9 significantly increased after treatment in a time dependent fashion. But the Bcl-2 protein was significantly down regulated after treatment with 123 and 164 μM concentrations of compound for 24 h (Fig. 7B). In western blotting analysis, release of cytochrome c was clearly more in A549 cells incubated with compound at 24 h (Fig. 8). The release of cytochrome c induces cleavage of caspase-9 which contributes to the activation of caspase-3. The intrinsic apoptosis signal pathway is the release of cytochrome c in mitochondria and the extrinsic pathway is the activation of death receptors such as TNF receptor, Fas or TNFa-related apoptosis inducing ligand (TRAIL) receptors. These death receptors are activated by cellular stress or death signals, and lead to the recruitment of Fas associated death domain (FADD) and death domain (DD) binding, which cause the activation of caspase-8 and caspase-10 [41–43]. Our results showed that cleavage of caspase-9 and caspase-3 were up-regulated by a p53 dependent pathway (Fig. 9). Caspase-3 is considered as a key protease that is activated during the early stages of apoptosis. Caspases are activated in a sequential cascade of cleavages from their inactive forms and the active caspase-3 proteolytically cleaves and activates other caspases and other relevant target molecules in the cytoplasm or nucleus. The process of cell death may involve the release of cytochrome c from the mitochondria which subsequently causes apoptosis by activation of the caspases. Together, these data suggest a linear and specific activation cascade between caspase-9 and caspase-3 in response to cytochrome c released from the mitochondria. Activation of caspase-9, in turn, cleaves effector caspases such as caspase-3, -6, and -7 [44]. Then the effector caspases cleave their target proteins and culminate in the orderly demise of the cell. In this pathway of apoptosis, caspase-3 and caspase-9 may be the most important as their activities influence the process of apoptosis as well as the type of cell death [45–47]. Caspase-3 then can cleave a series of proteins such as PARP, a DNA repair enzyme, nuclear lamins, gelsolin, and fodrin [48]. In the mitochondria, the tBid efficiently activates Bax, initiating the release of cytochrome c and mitochondrial dysfunction. This alternative is a crosstalk between the receptor and mitochondria mediated pathways that can amplify caspase activation necessary for apoptosis. In fact, more recent studies focus on multiple signal transduction cascades

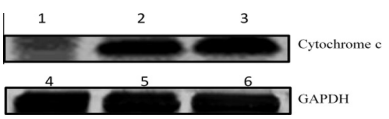


**Fig. 8.** Cytochrome c was detected by Western blotting analysis in A549 cells after treatment with flavonoid for 24 h: untreated samples lane 1, lane 2 – 123 μM, lane 3 – 164 μM and lane 4,5,6 control (GAPDH).

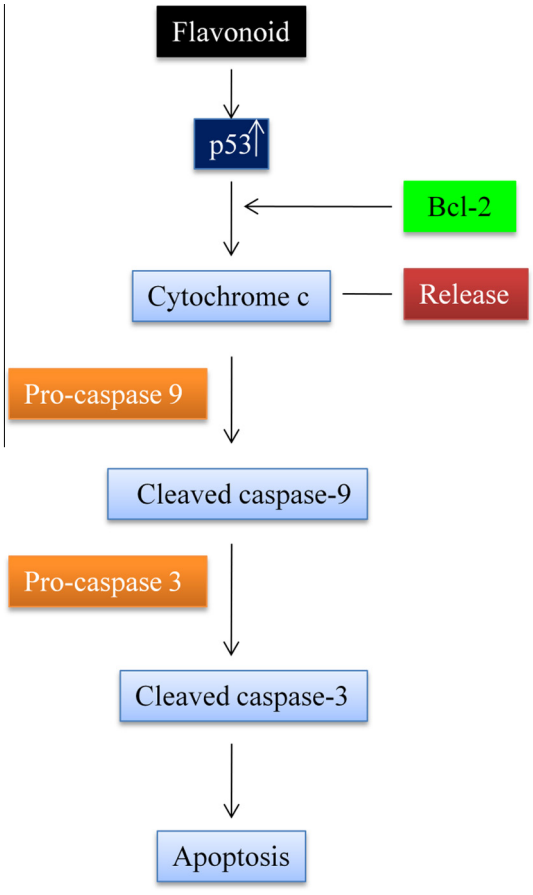


**Fig. 9.** A proposed model for isolated compound-induced apoptosis in A549 lung cancer cells. Compound induces apoptosis via activation of p53 and cytochrome c release caspase dependant pathway.

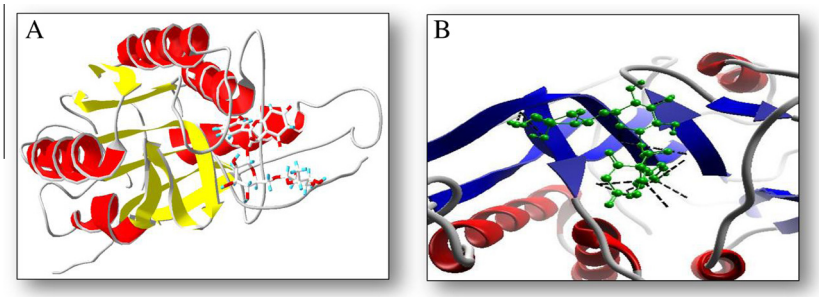


**Fig. 10.** Docking of quercetin-3-O-β-L-rhamnopyranosyl-(1 → 6)-β-D-glucopyranoside in caspase-3 (1QX3). (A and B) indicates the two and three dimensional interaction of compound-Casepase-3 (Pose view and PyMol viewer).

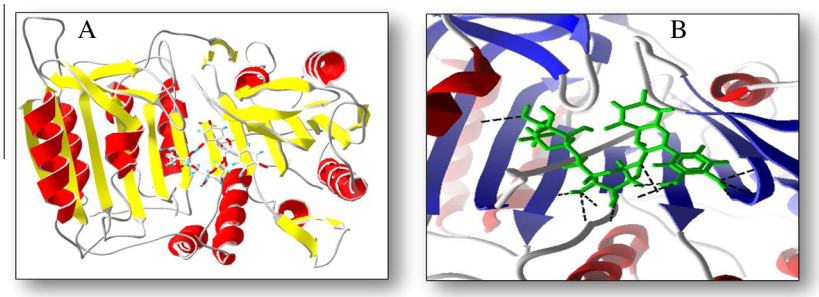


**Fig. 11.** Docking of quercetin-3-O-β-L-rhamnopyranosyl-(1 → 6)-β-D-glucopyranoside in caspase-9 (1JXQ). (A and B) indicates the two and three dimensional interaction of compound-Casepase-9 (Pose view and PyMol viewer).

that trigger cells to undergo apoptosis [49,50]. So we concluded that compound induced apoptosis in A549 cells via the activation of caspase dependent pathway through cytochrome c release, caspase-9 triggered mitochondria pathway and caspase-3 mediated death receptor pathway. Various natural products including flavonoid derivatives, indole-3-carbinol (I3C), 3, 30-diindolylmethane (DIM), curcumin, (−)-epiglallocatechin-3-gallate, etc, have been reported as natural agents to inhibit cancer development through multiple cellular signaling [51]. Quercetin showed apoptosis in many types of cancer cell lines [52–56]. Previous studies showed that quercetin, the aglycone of the above compound, suppressed the synthesis of the Bcl-2 protein in different malignant tumor cell lines, including acute leukemia cell line HL-60 and chronic B-cell leukemia lines [57,58]. Lee et al. [59] reported that quercetin inhibited the expression of Cox-2 to induce apoptosis in both breast cancer and colon cancer cells. Quercetin could reduce the growth of diethylnitrosamine induced hepatocarcinoma when introduced intravenously to rats (8.98 mM/kg) once a week for 16 weeks [60]. Rutin compound showed antiviral, antiallergic, antiplatelet, anti-inflammatory, antitumor and antioxidant properties [61–63]. Rutin was found to have chemopreventative activity in several animal models including azoxymethane-induced colon tumorigenesis in mice and rats [64–66], dimethylbenz(a)anthracene (DMBA) and N-nitrosomethylurea-treated mammary glands of rats and DMBA-treated skin cancer [67]. Rutin also showed cell cycle arrest and induced apoptosis in many types of human cancer cell lines [68–77].

### 3.3. Molecular docking properties

The crystal structures of caspase-3 (1QX3) and caspase-9 (1JXQ) were downloaded from PDB database. The compound showed 9 hydrogen bonds interactions with caspase-3 and the following amino acids such as Gly122, His121, Tyr204, Gln161, Ser120, Arg64, Thr166, Ser205 and Cys163 respectively. The lowest free energy score after docking was −195.446. The energy before and after docking was found to be −204.175 kcal and −204.176 kcal, respectively (Fig. 10A and B). The crystal structure of caspase-9 (1JXQ) was downloaded from PDB database. The molecule showed 7 hydrogen bonds interactions with caspase-9 with the following amino acids such as Met386, Pro387, Thr323, Asn263, Gln385, Ala284 and Gly286 respectively. The lowest free energy score after docking was −212.264. The protein structure was optimized using Nelder–Mead Simplex method. The energy before and after docking was found to be −219.252 kcal and −219.736 kcal, respectively (Fig. 11A and B). This study explored the use of the active form of caspase-3 for the detection of apoptotic events. This protease has been implicated as an "effector" caspase associated with the initiation of the "death cascade" and is therefore an important marker of the cell's entry point into the apoptotic signaling pathway [78]. Caspase-3 is activated by the upstream caspase-8 and caspase-9, and since it serves as a convergence point for different signaling pathways, it is well suited as a read-out in an apoptosis assay.

## 4. Conclusion

Quercetin-3-O-β-L-rhamnopyranosyl-(1 → 6)-β-D-glucopyranoside was isolated from *Streptomyces* sp. (ERINLG-4) and tested against A549 lung cancer cell line. The compound showed prominent cytotoxic activity at 123 and 164 μM. After isolated compound treatment DNA was fragmented and apoptotic body was visualized using confocal microscope. Bcl-2, p53, pro-caspases, caspase-3, caspase-9 and cytochrome c release were detected by western blotting analysis after compound treatment. Activities of caspase-3 and caspase-9 were gradually increased after the addition of compound. But Bcl-2 protein was down regulated after treatment of flavonoid. The level of anticancer potential was studied by automated docking of ligands to the binding sites of caspase-3 and caspase-9. The results revealed that the compound showed minimum binding energy which indicated its strong

affinity towards caspase-3 and caspase-9 proteins. This molecular mechanism for apoptotic effect of compound on A549 lung carcinoma cells is a first report and suggests that this compound may be used as a preventive and therapeutic agent against lung cancer.

## Conflict of Interest

The authors declare that there are no conflicts of interest.

## Transparency Document

The Transparency document associated with this article can be found in the online version.

## Acknowledgement

The authors would like to extend their sincere appreciation to the Deanship of Scientific Research at King Saud University for its funding of this research through the Research Group project No. RGP-VPP-213.

## Appendix A. Supplementary data

Supplementary data associated with this article can be found, in the online version, at http://dx.doi.org/10.1016/j.cbi.2014.09.019.

## References

[1] World Health Organization, <http://www.who.int/mediacentre/factsheets/fs297/en/>, Cancer Fact sheet N297, 2008.
[2] M. Takizawa, R.R. Colwell, R.T. Hell, Isolation and diversity of actinomycetes in the Chesapeake bay, Appl. Environ. Microbiol. 59 (1993) 997–1002.
[3] S.T. Williams, M. Goodfellow, G. Alderson, E.M. Wllington, P.H. Sneath, M.J. Sacki, Numerical classification of *Streptomyces* and related genera, J. Gen. Microbiol. 129 (1983) 1747–1813.
[4] B.K. Hwang, S.J. Ahn, S.S. Moon, Production, purification and anti-fungal activity of the antibiotic nucleoside, tuberecidine, produced by *Streptomyces violaceonig*, Can. J. Bot. 72 (1994) 480–485.
[5] S. Miyadoh, Research on antibiotic screening in Japan over the last decade: a producing microorganisms approach, Actinomycetologica 9 (1993) 100–106.
[6] R.H. Chen, D.M. Brady, D. Smith, A.W. Murray, H.G. Hardwick, The spindle checkpoint of budding yeast depends on a tight complex between the Mad1 and Mad2 proteins, Mol. Biol. Cell 10 (1999) 2607–2618.
[7] X. Liu, C.N. Kim, J. Yang, R. Jemmerson, X. Wang, Induction of apoptotic program in cell-free extracts: requirement for dATP and cytochrome c, Cell 86 (1996) 147–157.
[8] J.M. Zapata, K. Pawlowski, E. Haas, C.F. Ware, A. Godzik, J.C. Reed, A diverse family of proteins containing tumor necrosis factor receptor-associated factor domains, J. Biol. Chem. 276 (2001) 24242–24252.
[9] D. Hockenbery, G. Nunez, C. Milliman, R.D. Schreiber, S.J. Korsmeyer, Bcl-2 is an inner mitochondrial membrane protein that blocks programmed cell death, Nature 348 (1990) 334–336.
[10] N.A. Thornberry, Y. Lazebnik, Caspases: enemies within, Science 281 (1998) 1312–1316.
[11] M. Mancini, D.W. Nicholson, S. Roy, N.A. Thornberry, E.P. Peterson, L.A. CasciolaRosen, A. Rosen, The caspase-3 precursor has a cytosolic and mitochondrial distribution: implications for apoptotic signalling, J. Cell Biol. 140 (1998) 1485–1495.
[12] W.S. El-Deiry, Regulation of p53 downstream genes, Semin. Cancer Biol. 8 (1998) 345–357.
[13] S. Roy, M. Kaur, C. Agarwal, M. Tecklenburg, R.A. Sclafani, R. Agarwal, P21 and p27 induction by silibinin is essential for its cell cycle arrest effect in prostate carcinoma cells, Mol. Cancer Ther. 6 (2007) 2696–2707.
[14] S. Safe, S. Papineni, S. Chintharlapalli, Cancer chemotherapy with indole-3-carbinol, bis(30-indolyl)methane and synthetic analogs, Cancer Lett. 269 (2008) 326–338.
[15] J.R. Weng, C.H. Tsai, S.K. Kulp, C.S. Chen, Indole-3-carbinol as a chemopreventive and anti-cancer agent, Cancer Lett. 262 (2008) 153–163.
[16] M.L. AgarwalL, W.R. Taylor, M.V. Chernov, O.B. Chernova, G.R. Stark, The p53 network, J. Biol. Chem. 273 (1998) 1–4.
[17] D.A. Liebermann, B. Hoffman, D. Vesely, P53 induced growth arrest versus apoptosis and its modulation by survival cytokines, Cell Cycle 6 (2007) 166–170.
[18] J.L. Shirling, D. Gottlieb, Methods for characterization of *Streptomyces* species, Int. J. Syst. Bacteriol. 16 (1966) 313–340.
[19] C. Balachandran, V. Duraipandiyan, K. Balakrishna, S. Ignacimuthu, Petroleum and polycyclic aromatic hydrocarbons (PAHs) degradation and naphthalene metabolism in *Streptomyces* sp. (ERI-CPDA-1) isolated from oil contaminated soil, Bioresour. Technol. (2012) 83–90.
[20] C. Balachandran, Y. Arun, V. Duraipandiyan, S. Ignacimuthu, K. Balakrishna, N.A. Al-Dhabi, Antimicrobial and cytotoxicity properties of 2,3-dihydroxy-9,10-anthraquinone isolated from *Streptomyces galbus* (ERINLG-127), Appl. Biochem. Biotechnol. 172 (2014) 3513–3528.
[21] K. Tamura, J. Dudley, M. Nei, S. Kumar, MEGA4: molecular evolutionary genetics analysis (MEGA) software version 4.0, Mol. Biol. Evol. 24 (2007) 1596–1599.
[22] C. Balachandran, V. Duraipandiyan, K. Balakrishna, R. Lakshmi Sundaram, A. Vijayakumar, S. Ignacimuthu, N.A. Al-Dhabi, Synthesis and medicinal properties of plant-derived vilangin, Environ. Chem. Lett. 11 (2013) 303–308.
[23] H. Akiyama, M. Endo, T. Matsui, I. Katsuda, N. Emi, Y. Kawamoto, T. Koike, H. Beppu, Agaritine from Agaricus blazei Murrill induces apoptosis in the leukemic cell line U937, Biochim. Biophys. Acta 2011 (1810) 519–525.
[24] C. Hee-Sook, C. Min-Chul, L. Hee Gu, Y. Do-Young, Indole-3-carbinol induces apoptosis through p53 and activation of caspase-8 pathway in lung cancer A549 cells, Food Chem. Toxicol. 48 (2010) 883–890.
[25] P. Chomczynski, N. Sacchi, Single-step method of RNA isolation by acid guanidinium thiocyanate-phenol-chloroform extraction, Anal. Biochem. (1987) 156–159.
[26] D. Robert, W. Barber Dan, A. Harme Robert, J. Coleman Brian, Clark GAPDH as a housekeeping gene: analysis of GAPDH mRNA expression in a panel of 72 human tissues, Physiol. Genomics (2005) 1094–8341.
[27] A.T. Laurie, R.M. Jackson, Q-SiteFinder: an energy-based method for the prediction of protein-ligand binding sites, Bioinformatics (2005) 1908–1916.
[28] D.K. Gehlhaar, G. Verkhivker, P.A. Rejto, D.B. Fogel, L.J. Fogel, S.T. Freer, Docking conformationally flexible small molecules into a protein binding site through evolutionary programming, in: Proceedings of the Fourth International Conference on Evolutionary Programming, 1995, pp. 615–627.
[29] J.M. Yang, C.C. Chen, GEMDOCK: a generic evolutionary method for molecular docking, Proteins 55 (2004) 288–304.
[30] Z. Michalewicz, D.B. Fogel, How to Solve It: Modern Heuristics, Springer-Verlag, Berlin, 2000.
[31] M. Oskay, A.U. Tamer, C. Azeri, Antibacterial activity of some actinomycetes isolated from farming soils of Turkey, Afr. J. Biotechnol. 3 (2004) 441–446.
[32] H. Urakawa, K. Kita-Tsukamoto, K. Ohwada, Microbial diversity in marine sediments from Sagami Bay and Tokyo Bay, Japan, as determined by 16S rRNA gene analysis, Microbiology 145 (1999) 3305–3315.
[33] Yuanying Qi, Ailing Sun, Renmin Liu, Zhaoling Meng, Hongyan Xie, Isolation and purification of flavonoid and isoflavonoid compounds from the pericarp of *Sophora japonica* L. by adsorption chromatography on 12% cross-linked agarose gel media, J. Chromatogr. A 1140 (2007) 219–224.
[34] E.R. El-Sharkawy, A.A. Matloub, E.M. Atta, Cytotoxicity of new flavonoid compound isolated from *Farsetia aegyptia*, Int. J. Pharm. Sci. Invent. 2 (2013) 23–27.
[35] G. Galati, P.J.O. Brien, Potential toxicity of flavonoids and other dietary phenolics: significance for their chemopreventive and anticancer properties, Free Radical Biol. Med. 37 (2004) 287–303.
[36] Tzu-Chin Wu, Ying-Chihi Yang, Pei-Ru Huang, Yu-Der Wen, Shu-Lan Yeh, Genistein enhances the effect of trichostatin A on inhibition of A549 cell growth by increasing expression of TNF receptor-1, Toxicol. Appl. Pharmacol. 262 (2012) 247–254.
[37] T. Banerjee, A. Van der Vliet, V.A. Ziboh, Down regulation of COX-2 and iNOS by amentoflavone and quercetin in A549 human lung adenocarcinoma cell line, Prostaglandins Leukot. Essent. Fatty Acids 66 (2002) 485–492.
[38] I.K. Wang, S.Y. Lin-Shiau, J.K. Lin, Induction of apoptosis by apigenin and related flavonoids through cytochrome c release and activation of caspase-9 and caspase-3 in leukaemia Hl-60 cells, Eur. J. Cancer 35 (1999) 1517–1525.
[39] S. Matoba, K. Ju-Gyeong, W.D. Patino, A. Wragg, M. Boehm, O. Gavrilova, P.J. Hurley, F. Bunz, M. Paul, H. wang, p53 Regulates mitochondrial respiration, Science 312 (2006) 1650.
[40] A. Vazquez, E.E. Bond, A.J. Levine, G.L. Bond, The genetics of the p53 pathway, apoptosis and cancer therapy, Nat. Rev. Drug Discovery 7 (2008) 979–987.
[41] S.K. Kelley, A. Ashkenazi, Targeting death receptors in cancer with Apo2L/TRAIL, Curr. Opin. Pharmacol. 4 (2004) 333–339.
[42] A. Thorburn, Death receptor-induced cell killing, Cell. Signal. 16 (2004) 139–144.
[43] S. Wang, W.S. El-Deiry, TRAIL and apoptosis induction by TNF-family death receptors, Oncogene 22 (2003) 8628–8633.
[44] D.W. Nicholson, N.A. Thornberry, Caspases: killer proteases, Trends Biochem. Sci. 22 (1997) 299–306.
[45] A.M. Martelli, L. Manzoli, L. Cocco, Nuclear inositides: facts and perspectives, Pharmacol. Ther. 101 (2004) 47–64.
[46] C.A. Coelho, R.E. McHugh, M. Boyle, Semantic feature analysis as a treatment for aphasic dysnomia: a replication, Aphasiology 14 (2000) 133–142.
[47] T.S. Zheng, S. Hunot, K. Kuida, T. Momoi, A. Srinivasan, W.D. Nicholson, Y.L. Richard Flavell, Deficiency in caspase-9 or caspase-3 induces compensatory caspase activation, Nature 6 (2000) 1241–1247.
[48] H.Y. Chang, X. Yang, Proteases for cell suicide: regulation and functions of caspases, Microbiol. Mol. Biol. Rev. 64 (2000) 821–846.
[49] G. Kroemer, J.M. Seamus, Caspase-independent cell death, Nat. Med. 11 (2005) 725–730.

[50] Haimovitz-friedman, Radiation-induced signal-transduction and stress-response, Radiat. Res. 150 (1998) 102–108.
[51] N.K. Sarkar, Y. Kim, A. Grove, Rice sHsp genes: genomic organization and expression profiling under stress and development, BMC Genomics 10 (2009) 393.
[52] J. Jakubowicz-Gil, E. Langner, I. Wertel, T. Piersiak, W. Rzeski, Temozolomide, quercetin and cell death in the MOGGCCM astrocytoma cell line, Chem. Biol. Interact. 188 (2010) 190–203.
[53] S. Devipriya, V. Ganapathy, C.S. Shyamaladevi, Suppression of tumor growth and invasion in 9,10 dimethyl benz(*a*) anthracene induced mammary carcinoma by the plant bioflavonoid quercetin, Chem. Biol. Interact. 162 (2006) 106–113.
[54] Y.J. Kim, E.B. Jung, S.J. Seo, K.H. Park, M.W. Lee, C.S. Lee, Quercetin-3-O-(2″-galloyl)-α-l-rhamnopyranoside prevents TRAIL-induced apoptosis in human keratinocytes by suppressing the caspase-8 and Bid-pathways and the mitochondrial pathway, Chem. Biol. Interact. 204 (2013) 144–152.
[55] E.H. Rodgers, M.H. Grant, The effect of the flavonoids, quercetin, myricetin and epicatechin on the growth and enzyme activities of MCF7 human breast cancer cells, Chem. Biol. Interact. 116 (1998) 213–228.
[56] A.B. Granado-Serrano, M.A. Martín, L. Bravo, L. Goya, S. Ramos, Quercetin modulates Nrf2 and glutathione-related defenses in HepG2 cells: involvement of p38, Chem. Biol. Interact. 195 (2012) 154–164.
[57] D. Xiao, Z.L. Gu, S.P. Zhu, Quercetin down-regulated bcl-2 gene expression in human leukemia HL-60 cells, Zhongguo Yao Li Xue Bao 19 (1998) 551–553.
[58] A. König, G.K. Schwartz, R.M. Mohammad, A. Al-Katib, J.L. Gabrilove, The novel cyclin-dependent kinase inhibitor flavopiridol downregulates Bcl-2 and induces growth arrest and apoptosis in chronic B-cell leukemia lines, Blood 90 (1997) 4307–4312.
[59] Y.K. Lee, S.Y. Park, Y.M. Kim, W.S. Lee, O.J. Park, AMP kinase/cyclooxygenase-2 pathway regulates proliferation and apoptosis of cancer cells treated with quercetin, Exp. Mol. Med. 41 (2009) 201–207.
[60] A.K. Mandal, S. Das, M. Mitra, R.N. Chakrabarti, M. Chatterjee, N. Das, Vesicular flavonoid in combating diethylnitrosamine induced hepatocarcinoma in rat model, J. Exp. Ther. Oncol. 7 (2008) 123–133.
[61] S.H. Nile, S.W. Park, Edible berries: review on bioactive components and their effect on human health, Nutrition (2013).
[62] H. Hoensch, R. Oertel, Anti-inflammatory effects of teaflavonoids, Dtsch. Med. Wochenschr. 137 (2012) 2738–2740.
[63] M.S. Geybels, B.A. Verhage, I.C. Arts, F.J. van Schooten, R.A. Goldbohm, P.A. van den Brandt, Dietary flavonoid intake, black tea consumption, and risk of overall and advanced stage prostate cancer, Am. J. Epidemiol. 177 (2013) 1388–1398.
[64] E.E. Deschner, J.F. Ruperto, G.Y. Wong, H.L. Newmark, The effect of dietary quercetin and rutin on AOM-induced acute colonic epithelial abnormalities in mice fed a high-fat diet, Nutr. Cancer 20 (1993) 199–204.
[65] Y. Matsukawa, H. Nishino, Y. Okuyama, T. Matsui, T. Matsumoto, S. Matsumura, Y. Shimizu, Y. Sowa, T. Sakai, Effects of quercetin and/or restraint stress on formation of aberrant crypt foci induced by azoxymethane in rat colons, Oncology 54 (1997) 118–121.
[66] T. Tanaka, K. Kawabata, S. Honjo, H. Kohno, M. Murakami, R. Shimada, K. Matsunaga, Y. Yamada, M. Shimizu, Inhibition of azoxymethane-induced aberrant crypt foci in rats by natural compounds, caffeine, quercetin and morin, Oncol. Rep. 6 (1999) 1333–1340.
[67] A.K. Verma, J.A. Johnson, M.N. Gould, M.A. Tanner, Inhibition of 7, 12-dimethylbenz(a)anthracene- and N-nitrosomethylureainduced rat mammary cancer by dietary flavonol quercetin, Cancer Res. 48 (1988) 5754–5758.
[68] F. Pu, K. Mishima, N. Egashira, K. Iwasaki, T. Kaneko, T. Uchida, K. Irie, D. Ishibashi, H. Fujii, K. Kosuna, et al., Protective effect of buckwheat polyphenols against long-lasting impairment of spatial memory associated with hippocampal neuronal damage in rats subjected to repeated cerebral ischemia, J. Pharmacol. Sci. 94 (2004) 393–402.
[69] N. Kamalakkannan, P. Stanely Mainzen Prince, Rutin improves the antioxidant status in streptozotocin-induced diabetic rat tissues, Mol. Cell. Biochem. 293 (2006) 211–219.
[70] T. Koda, Y. Kuroda, H. Imai, Protective effect of rutin against spatial memory impairment induced by trimethyltin in rats, Nutr. Res. 28 (2008) 629–634.
[71] C. La Casa, I. Villegas, C. Alarcon de la Lastra, V. Motilva, M.J. Martin Calero, Evidence for protective and antioxidant properties of rutin, a natural flavone, against ethanol induced gastric lesions, J. Ethnopharmacol. 71 (2000) 45–53.
[72] G. Gong, Y. Qin, W. Huang, S. Zhou, X. Yang, D. Li, Rutin inhibits hydrogen peroxide-induced apoptosis through regulating reactive oxygen species mediated mitochondrial dysfunction pathway in human umbilical vein endothelial cells, Eur. J. Pharmacol. 628 (2010) 27–35.
[73] J.P. Lin, J.S. Yang, C.C. Lu, J.H. Chiang, C.L. Wu, J.J. Lin, H.L. Lin, M.D. Yang, K.C. Liu, T.H. Chiu, et al., Rutin inhibits the proliferation of murine leukemia WEHI-3 cells in vivo and promotes immune response in vivo, Leuk. Res. 33 (2009) 823–828.
[74] H. Chen, Q. Miao, M. Geng, J. Liu, Y. Hu, L. Tian, J. Pan, Y. Yang, Anti-tumor effect of rutin on human neuroblastomacell lines through inducing G2/M cell cycle arrest and promoting apoptosis, The Scientific World Journal (2013) 8 (Hindawi Publishing Corporation).
[75] S.R. Volate, D.M. Davenport, S.J. Muga, M.J. Wargovich, Modulation of aberrant crypt foci and apoptosis by dietary herbal supplements (Quercetin, curcumin, silymarin, ginseng and rutin), Carcinogenesis 26 (2005) 1450–1456.
[76] C. Carrasco-Pozo, M.L. Mizgier, H. Speisky, M. Gotteland, Differential protective effects of quercetin, resveratrol, rutin and epigallocatechin gallate against mitochondrial dysfunction induced by indomethacin in Caco-2 cells, Chem. Biol. Interact. 195 (2012) 199–205.
[77] S. Yeh, W. Wang, C. Huang, M. Hu, Flavonoids suppresses the enhancing effect of β-carotene on DNA damage induced by 4-(methylnitrosamino)-1-(3-pyridyl)-1-butanone (NNK) in A549 cells, Chem. Biol. Interact. 160 (2006) 175–182.
[78] Y. Tsujimoto, J. Cossman, E. Jaffe, C.M. Croce, Involvement of the bcl-2 gene in human follicular lymphoma, Science 228 (1985) 1440–1443.